ACS Macro Letters

Letter

pubs.acs.org/macroletters

Facile Synthesis of a Phosphorylcholine-Based Zwitterionic Amphiphilic Copolymer for Anti-Biofouling Coatings

Kellie Seetho,[†] Shiyi Zhang,[†] Kevin A. Pollack,[†] Jiong Zou,[†] Jeffery E. Raymond,[†] Edgar Martinez,[‡] and Karen L. Wooley*,[†]

[†]Departments of Chemistry, Chemical Engineering and Materials Science and Engineering, Laboratory for Synthetic–Biologic Interactions, Texas A&M University, College Station, Texas 77842, United States

[‡]Beckman Coulter Particle Characterization Laboratory, MS 22-B02, Miami, Florida 33196, United States

Supporting Information

ABSTRACT: An antibiofouling polymer coating, combined with both zwitterionic and amphiphilic features, is engineered by a two-step modification of a commodity polymer. The surface properties of the resultant polymer coating can be easily tuned by varying the extent of cross-linking in the network. Higher antibiofouling efficiency was observed for these surfaces vs. an elastomeric polydimethylsiloxane standard (Sylgard 184) against the adsorption of biomacromolecules and a marine fouling organism (*Ulva* zoospores) has been demonstrated. This design establishes a platform for the achievement of functionalized amphiphilic zwitterionic copolymers from relatively inexpensive starting materials via simple chemical manipulations.

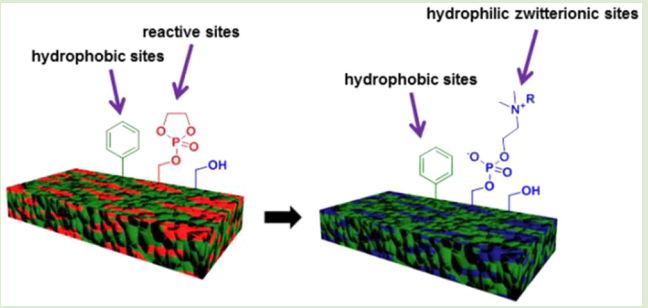

Biofouling is a persistent global problem that is detrimental to the shipping industry from both economical and environmental standpoints.[1−3] The U.S. Navy alone, which accounts for less than half a percent of the world's shipping industry, spends $180−260 M USD per year in fuel and hull cleaning costs due to fouling.[4] Additionally, fouling poses a significant threat to the environment as invasive organisms on ship hulls are transported into foreign waters creating ecological imbalances.[5] In the 1960s, marine paints containing tributyltin (TBT) were used to combat biofouling through leaching of the TBT from the paint.[6] Although the strategy to incorporate organotin additives into marine paints was highly effective in resisting biofoulers, it has also been extremely harmful to the marine wildlife.[7] Cuprous oxides have also been used as an antibiofouling agent, but still pose similar detrimental effects to the marine environment.[8] The introduction of toxic agents into marine paints has led to criticisms of the usage of biocide additives and has resulted in the eventual banning of TBT by the International Maritime Organization (IMO).[9] The lack of nontoxic and effective alternatives to these toxic organotin and cuprous oxides calls for immediate attention, targeting more efficient and environmentally benign solutions to combat biofouling.

Polymeric materials have been investigated heavily as environmentally benign antibiofouling replacements for ship hull coatings to reduce fuel consumption, hull cleaning costs, and the invasion of nonindigenous species.[10−13] A number of polymers has been explored as antibiofouling coatings including hydrophobic polymers, such as silicone elastomers[10] and fluoropolymers,[11] hydrophilic polymers, such as poly(ethylene glycol) (PEG),[12] and zwitterionic polymers.[13] Although the various polymers display antibiofouling characteristics, with silicone elastomers and fluoropolymers already commercialized as nontoxic antibiofouling coatings, there remains a drawback using single component systems as many biofoulers release glycoprotein adhesives that have a higher affinity to either a hydrophobic or hydrophilic surface.[14,15] Hence, amphiphilic polymer coatings with optimal nanoscale heterogeneity of hydrophilic domains, usually PEG, and hydrophobic domains have been investigated and demonstrated by several groups in the field to be more effective antibiofouling coatings than only a single polymeric component.[14,16−19] Furthermore, zwitterionic polymer coatings have shown promising antibiofouling characteristics due to a hydration layer formed around the zwitterionic polymers through electrostatic interactions and hydrogen bonding that are both energetically and kinetically unfavorable for proteins to disrupt.[13,20−23] Although several amphiphilic and zwitterionic systems are currently being investigated as nontoxic antibiofouling coating replacements, individually, few systems incorporate zwitterions as the hydrophilic component in an amphiphilic design.[23,24] Herein, we present a novel strategy that utilizes simple chemistry to modify a commercially available polymer and then grafts it onto

Received: December 19, 2014
Accepted: April 15, 2015
Published: April 17, 2015

DOI: 10.1021/mz500818c
ACS Macro Lett. 2015, 4, 505−510

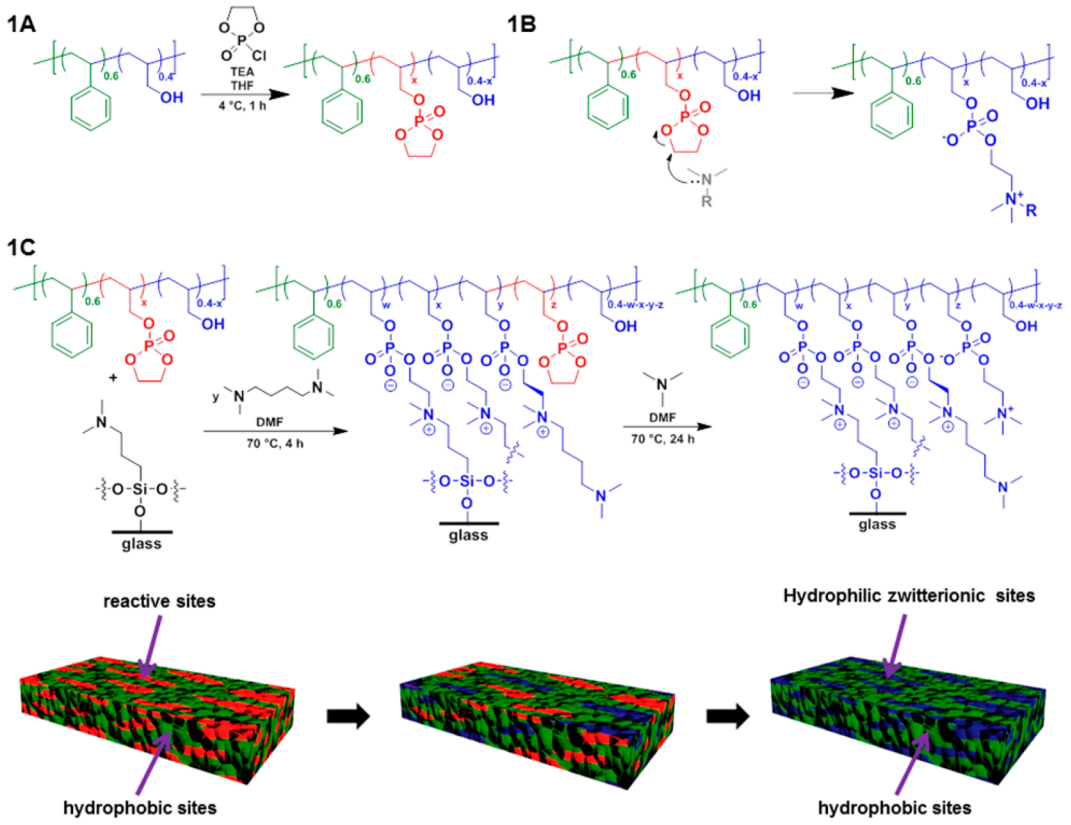

Figure 1. (A) Synthesis of SAP from SAA. (B) Mechanism for the ring opening of the phosphotriester units upon attack by a tertiary amine. (C) Schematic illustration of the preparation of different extents of cross-linked amphiphilic antibiofouling coatings on silanized substrates that present sterically nonhindered tertiary amines on the surface.

a substrate to form an amphiphilic polymer coating, in which the hydrophilic component is composed of zwitterionic units.

Our strategy to develop a simple chemical approach to produce an amphiphilic zwitterionic polymer coating from a commercially available polymer employed poly(styrene-*co*-allyl alcohol) (SAA) copolymer, which is widely used in ink and paint and involved the installation of reactive cyclic phosphotriester functionalities to allow for incorporation of zwitterionic groups, covalent attachment to a substrate, and cross-linking reactions (Figure 1). Even when purchased in small research quantities, this functional copolymer is relatively inexpensive, <$200/kg. The randomly distributed reactive hydroxyl groups on SAA were allowed to undergo reaction with 2-chloro-2-oxo-1,3,2-dioxaphospholane (COP; Figure 1A) under basic conditions to form poly(styrene-*co*-allyl phospholane) (SAP) copolymer, while the hydrophobic styrenyl groups were left unmodified to be used to create hydrophobic domains on the surfaces of the coatings. The resonance frequencies of the methylene protons of the hydroxymethyl functionalities shifted downfield upon formation of the cyclic phosphotriester side chain functionalities; however, there was significant overlap with the proton signals of the five-membered rings, which prevented quantitative determination of the extent of reaction by ^{1}H NMR spectroscopy (Figure S1). ^{13}C NMR spectroscopy allowed for confirmation that the reaction had proceeded, by having some level of distinction of the downfield-shifted methylene carbon signals, resonating broadly at 69−70 and 70−74 ppm), relative to the five-membered ring carbons (61−68 ppm); however, the starting hydroxymethyl methylene carbon signals overlapped (62−64 and 64−69 ppm), again, preventing quantitative determination of the extent of conversion of the hydroxyl methyl groups to cyclic phosphotriester moieties (Figure S2). Although ^{1}H and ^{13}C NMR spectra could not be used to ascertain complete conversion of the alcohol units in SAA to phosphotriester units in SAP, the disappearance of the infrared absorbance band associated with the hydroxyl stretch at 3100−3500 cm^{-1} in SAP suggested that most of the alcohols were converted to phosphotriester units (Figure S3). The highly reactive phosphotriester is able to react readily with tertiary amines to form phosphorylcholine (Figure 1B), which was deliberately chosen in our system because phosphorylcholine mimics the chemical structure of the outer cell membrane and has been shown to resist protein adhesion more readily than other zwitterions, such as sulfobetaines.[25−31] This chemistry permits the covalent incorporation of various functionalities or enhancement of cross-linking through the modification of the R group on the tertiary amine (Figure 1B). Similarly, substrates functionalized with tertiary amine can also allow the attachment of the polymer onto the substrate without the use of adhesives. SAA was converted into SAP with high yield through a one-step esterification reaction, followed by simple filtration and washing. SAP was then mixed with a difunctional tertiary amine, *N*,*N*,*N*′,*N*′-tetramethyl-1,4-butanediamine (TMBD), to form nominally 0, 25, and 50% cross-linked amphiphilic zwitterionic coatings, which refers to the maximum amount of cross-linking between the amines and phosphotriester units based upon their stoichiometries. The coatings were prepared by a solution deposition method on silanized glass substrates that presented tertiary amines on the surface, followed by treatment with trimethylamine to convert

DOI: 10.1021/mz500818c
ACS Macro Lett. 2015, 4, 505−510

the remaining phosphotriester units into phosphorylcholine units (Figure 1C).

The thicknesses of the 0, 25, and 50% cross-linked amphiphilic zwitterionic coatings were measured by calipers to be about 33 ± 1, 43 ± 1, and 46 ± 1 μm, respectively. As expected, the thickness increased with the presence of the TMBD cross-linker, likely due to a combination of the increased total mass of material and the more effective covalent attachment of SAP polymers within the networks and with connectivity to the substrate.

The coatings were characterized by X-ray photoelectron spectroscopy (XPS) to study the surface chemical compositions. In the scenario of full conversion of phosphotriester units into phosphorylcholine units, the nitrogen to phosphorus N/P ratio would be 1:1, due to a mechanism in which one lone pair on the nitrogen atom opens one phosphotriester five-membered ring. The 0% cross-linked coating resulted in a calculated N/P ratio of 0.8 indicating about 80% conversion efficiency (Table 1). Upon diamino-based cross-linking, the expected N/P ratio was observed, in which the 25 and 50% cross-linked coatings had N/P ratios of 1.0 and 1.1, respectively. The N/P value greater than 1 may be attributed to an increasing number of residual dangling amines from TMBD that did not react with the phosphotriester units. Thus, the N/P ratio of the higher cross-linked coatings would be able to exceed 1, due to TMBD molecules being attached onto the coating only from one single terminus. The N/P ratios close to the theoretical 1.0 suggest that the installation of the zwitterionic features on the modified surfaces was successful.

Table 1. Surface Chemical Composition of 0, 25, and 50% Cross-Linked Amphiphilic Zwitterionic Polymer Surfaces Calculated from XPS Spectra[a]

coatings	O (%)	N (%)	C (%)	P (%)	N/P
0% cross-linked	18.2 ± 0.1	1.3 ± 0.1	78.8 ± 0.1	1.7 ± 0.1	0.8
25% cross-linked	14.4 ± 0.7	2.3 ± 0.5	81.1 ± 0.2	2.2 ± 0.02	1.0
50% cross-linked	11.7 ± 0.7	1.8 ± 0.8	84.8 ± 2	1.6 ± 0.1	1.1

[a]Three areas were measured on each sample.

Atomic force microscopy (AFM) was used to investigate the surfaces of the coatings in both the dry and water-swollen states (Figure 2). In the dry state, all coatings presented rough surfaces with randomly distributed topographical features. The 0% cross-linked coatings exhibited surfaces with the lowest R_{rms} and change in surface area (ΔA^2), generating the smoothest surfaces out of the three coatings, and they were also the thinnest, qualitatively, due to the reliance only on substrate conjugation for connection to the substrate. The 50% cross-linked coatings generated the next smoothest surface while the 25% cross-linked coatings were the roughest surfaces. The addition of TMBD into the formulations allowed for multilayer cross-linking coincident with covalent attachment to the substrate to afford the 25 and 50% cross-linked networks. It is hypothesized that the lower degree of cross-linking gave a dynamic, loosely cross-linked network that could undergo surface-buckling and display greater nanoscopic and microscopic roughnesses, resulting in an increased R_{rms} and ΔA^2 than the 0 or 50% cross-linked coatings. Recognizing that further studies were needed to probe the composition, structure, property behaviors, the coatings were then immersed in nanopure water for 12 h to provide for images in the water-swollen state. Overall, the water-swollen coatings displayed a lower R_{rms} and decrease in surface area, resulting in a smoother surface than their dry counterparts. The decreases in R_{rms} and ΔA^2 indicate that dynamic surface reorganization or increased water hydration had occurred on the surface of and possibly throughout the films.

The wettability of the coatings was studied by measuring the static water contact angle (Figure 2). All coatings exhibited relatively low static water contact angles (<25°) prewater immersion, which is indicative of their zwitterionic nature and affinity to water. Upon water immersion, an increase in static water contact angle of all the coatings was observed compared to their dry counter parts. The observation of the contraphilic effect displayed on all surfaces can most likely be attributed to a saturation of water in the film allowing zwitterions in the surface water interface to also be able to bury within the film.[32] The trend of higher cross-linked films exhibiting higher static

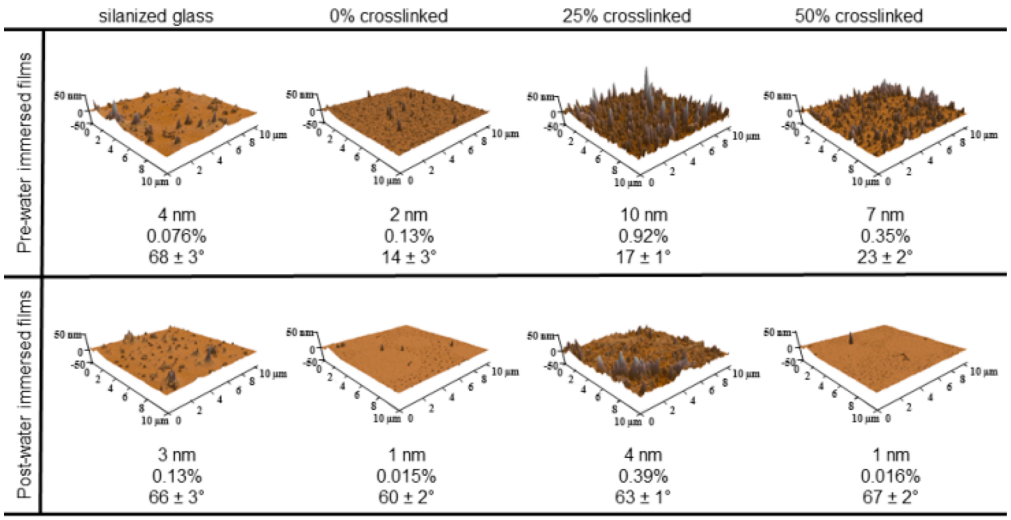

Figure 2. Atomic force microscopy images for amphiphilic zwitterionic coatings for both prewater and postwater swollen states with R_{rms}, ΔA^2, and static water contact angle values reported, respectively, with each image. Field of view for AFM renderings is 100 μm^2 with a 100 nm z-scale.

DOI: 10.1021/mz500818c
ACS Macro Lett. 2015, 4, 505−510

water contact angle was still observed with post water immersion films. The increase in static water contact angles for networks with a greater percentage of cross-linking could be attributed to the increase in hydrodynamic response to residual tertiary amine end groups that did not react with phosphotriester moieties on the surface. The trends observed by both AFM imaging and static water contact angle measurements suggested an ability to control the surface properties by modulating TMBD incorporation.

After the demonstration of their zwitterionic and amphiphilic features, the coatings were incubated with a nonspecific protein, bovine serum albumin (BSA) conjugated with Alexa Fluor 488 dye, to examine antibiofouling performance. By wide field fluorescence microscopy under identical imaging conditions, the histograms for the fluorescence intensities of the coatings before and after incubation for 1 h in BSA solution were obtained and compared to the controls: glass, silanized glass and glass coated with a commercially available silicone elastomer model Sylgard 184 (Figure 3). The average changes

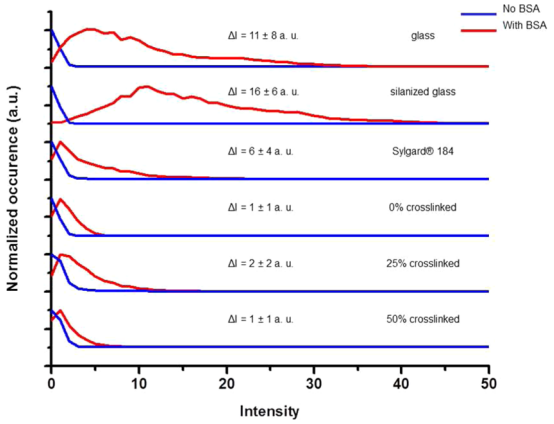

Figure 3. Histograms of fluorescence intensities of coatings/substrates before (blue curve) and after (red curve) BSA incubation, and calculated relative changes in fluorescence intensities.

in relative Alexa Fluor 488 intensities between pre- and post-BSA-exposed surfaces were calculated and presented along with the histograms. As more BSA was bound, a larger change in relative Alexa Fluor 488 intensity was expected. The histograms demonstrated that the amphiphilic zwitterionic coatings had changes in intensities no more than 2 au, while the changes in intensities for controls were ≥6 au The results indicated that amphiphilic zwitterionic coatings have a higher resistance to the adsorption of BSA than the controls (glass, silanized glass and Sylgard 184). The 0 and 50% cross-linked coatings both displayed slightly better antibiofouling resistances toward BSA adsorption (1 au) than the 25% cross-linked coating (2 au). The slightly higher resistance to BSA adsorption behavior for both the 0% and 50% cross-linked coatings could be accredited to the overall lower R_{rms} and ΔA^2 of the coatings in comparison to the 25% cross-linked coatings, a finding that was also observed by other groups.[33,34] In addition to a higher R_{rms} and surface area, the residual unreacted tertiary amines from TMBD in the 25 and 50% cross-linked coatings may also play a factor in the effectiveness of resistance to BSA adsorption.

With respect to the application of these amphiphilic zwitterionic coatings for antibiofouling applications in the marine environment, the abilities of the coatings to prevent settlement of *Ulva*, the most widespread hull fouling alga,[35] was tested by submerging the surfaces in an *Ulva* zoospore solution. Confocal microscopy was used to measure autofluorescence of chlorophyll present in zoospores that settled on the surfaces. The changes in relative fluorescence intensities between the coatings before and after zoospore settlement on the amphiphilic zwitterionic coatings were below 51 au, while the average changes for the controls were all above 190 au (Figure 4A). Although there was only a slight distinction among the

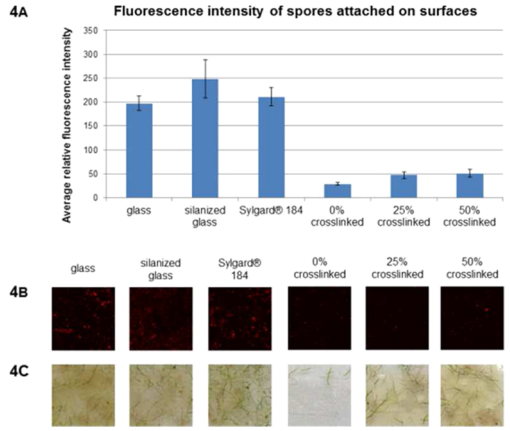

Figure 4. (A) Average relative chlorophyll fluorescence intensities results for tested coatings/substrates regarding settlement of *Ulva* zoospores. (B) Fluorescence images of the settlement of zoospores onto substrates. (C) Qualitative images of *Ulva* growth on substrates after 5 days. Size of each substrate is 1 cm^2.

fluorescence images of the amphiphilic zwitterionic coatings and the controls (Figure 4B), the calculated change in fluorescence intensities before and after zoospore settlement indicated that the amphiphilic zwitterionic coatings performed significantly better at resisting zoospore settlement than did the controls, including the PDMS elastomer coatings (Figure 4A,B), with all amphiphilic zwitterionic coatings having a 70% less susceptibility to *Ulva* fouling compared to the controls. The 0% cross-linked coatings were observed to be the most effective at preventing the settlement of zoospores among all coatings, with an average relative fluorescence intensity at approximately 30 au. Meanwhile, the average relative fluorescence intensities for 25% and 50% cross-linked coatings were calculated to be similar at approximately 50 au. The 0% cross-linked coating was able to resist the most zoospores, possibly due to its surface having the highest wettability among all coatings as illustrated by static water contact angle measurements. The zoospores that had settled on the coatings/substrates were also allowed to grow for qualitative measurements of *Ulva* fouling (Figure 4C) and the controls can be visually observed to be more fouled than were the amphiphilic zwitterionic coatings. In addition, the growth of the zoospores on the amphiphilic zwitterionic coatings also implied that our coatings are nontoxic.

The surface zeta potential of 0, 25, and 50% cross-linked coatings were measured to be −32.47, −22.50, and −54.39 mV, respectively. The negatively charged characteristic of the coatings could be in accordance to the ring opening of any remaining unreacted cyclic phosphotriester which did not react with an amine. Nanomaterials with phosphotriester moieties have also shown to exhibit negative characteristics.[36−38] Although the coatings showed negatively charged characteristics, it is hypothesized that the zwitterionic characteristics of

DOI: 10.1021/mz500818c
ACS Macro Lett. 2015, 4, 505−510

the phosphorylcholine in the coating decrease protein adsorption and microorganism adhesion.

A new facile strategy to achieve amphiphilic zwitterionic coatings has been developed, which starts from a commercially available relatively inexpensive polymer and allows for easy functionalization and cross-linking reactions. The wettabilities of the zwitterionic polymeric networks were controlled by varying the extent of cross-linking in the networks, which influenced the compositional profiles. AFM characterization suggested that the surface properties of our amphiphilic zwitterionic coatings could also be adjusted by tuning cross-linking extents. The amphiphilic zwitterionic coatings displayed superior antibiofouling performance at resisting both protein (BSA) and whole marine organism (*Ulva* zoospore) fouling, compared to glass substrates and commercialized antibiofouling silicone-based coatings.

With these promising initial antibiofouling results obtained for materials prepared by a straightforward synthetic approach, future directions will further explore the applicability of the current coatings, while also expanding the compositions, structures and properties. In particular, we are interested in controlled, quantitative laboratory and field tests of fouling performance, conducted against diverse types of marine organisms, with evaluation of the coatings surface characteristics before and after fouling has occurred to better map out the composition−structure−property−performance relationships. In addition, we are investigating expansion of the compositions, with inclusion of mixtures of amino components, coatings thicknesses, while also probing the durability and longevity under challenging conditions, including those resembling a marine environment.

■ ASSOCIATED CONTENT

Supporting Information

Experimental details. This material is available free of charge via the Internet at http://pubs.acs.org.

■ AUTHOR INFORMATION

Corresponding Author

*E-mail: wooley@chem.tamu.edu. Tel.: (979) 845-4077.

Notes

The authors declare no competing financial interest.

■ ACKNOWLEDGMENTS

This work was supported by the Office of Naval Research, Grant Nos. N00014-10-1-0527 and N00014-14-1-0082, and the Welch Foundation through the W. T. Doherty-Welch Chair in Chemistry, Grant No. A-0001. We would also like to acknowledge the Materials Characterization Facility at Texas A&M University for XPS instrumentation access and training.

■ REFERENCES

(1) Xiao, L.; Li, J.; Mieszkin, S.; Di Fino, A.; Clare, A. S.; Callow, M. E.; Callow, J. A.; Grunze, M.; Rosenhahn, A.; Levkin, P. A. *ACS Appl. Mater. Interfaces* **2013**, *5*, 10074−10080.

(2) Serrano, Â.; Sterner, O.; Mieszkin, S.; Zürcher, S.; Tosatti, S.; Callow, M. E.; Callow, J. A.; Spencer, N. D. *Adv. Funct. Mater.* **2013**, *23*, 5706−5718.

(3) Detty, M. R.; Ciriminna, R.; Bright, F. V.; Pagliaro, M. *Acc. Chem. Res.* **2014**, *47*, 678−687.

(4) Schultz, M. P.; Bendick, J. A.; Holm, E. R.; Hertel, W. M. *Biofouling* **2010**, *27*, 87−98.

(5) Yamaguchi, T.; Prabowo, R. E.; Ohshiro, Y.; Shimono, T.; Jones, D.; Kawai, H.; Otani, M.; Oshino, A.; Inagawa, S.; Akaya, T.; Tamura, I. *Biofouling* **2009**, *25*, 325−333.

(6) Howell, D.; Behrends, B. *Biofouling* **2006**, *22*, 401−410.

(7) Maguire, R. J. *Appl. Organomet. Chem.* **1987**, *1*, 475−498.

(8) Omae, I. *Appl. Organomet. Chem.* **2003**, *17*, 81−105.

(9) Yebra, D. M.; Kiil, S.; Dam-Johansen, K. *Prog. Org. Coat.* **2004**, *50*, 75−104.

(10) Schumacher, J. F.; Carman, M. L.; Estes, T. G.; Feinberg, A. W.; Wilson, L. H.; Callow, M. E.; Callow, J. A.; Finlay, J. A.; Brennan, A. B. *Biofouling* **2007**, *23*, 55−62.

(11) Andruzzi, L.; Hexemer, A.; Li, X.; Ober, C. K.; Kramer, E. J.; Galli, G.; Chiellini, E.; Fischer, D. A. *Langmuir* **2004**, *20*, 10498−10506.

(12) Prime, K. L.; Whitesides, G. M. *J. Am. Chem. Soc.* **1993**, *115*, 10714−10721.

(13) Zhang, Z.; Chao, T.; Chen, S.; Jiang, S. *Langmuir* **2006**, *22*, 10072−10077.

(14) Krishnan, S.; Wang, N.; Ober, C. K.; Finlay, J. A.; Callow, M. E.; Callow, J. A.; Hexemer, A.; Sohn, K. E.; Kramer, E. J.; Fischer, D. A. *Biomacromolecules* **2006**, *7*, 1449−1462.

(15) Schlip, S. K. A.; Rosenhahn, A.; Grunze, M.; Pettitt, M. E.; Callow, M. E.; Callow, J. A. *Biointerphases* **2007**, *2*, 143−150.

(16) Wang, Y.; Betts, D. E.; Finlay, J. A.; Brewer, L.; Callow, M. E.; Callow, J. A.; Wendt, D. E.; DeSimone, J. M. *Macromolecules* **2011**, *44*, 878−885.

(17) Park, D.; Weinman, C. J.; Finlay, J. A.; Fletcher, B. R.; Paik, M. Y.; Sundaram, H. S.; Dimitriou, M. D.; Sohn, K. E.; Callow, M. E.; Callow, J. A.; Handlin, D. L.; Willis, C. L.; Fischer, D. A.; Kramer, E. J.; Ober, C. K. *Langmuir* **2010**, *26*, 9772−9781.

(18) Pollack, K. A.; Imbesi, P. M.; Raymond, J. E.; Wooley, K. L. *ACS Appl. Mater. Interfaces* **2014**, *6*, 19265−19274.

(19) van Zoelen, W.; Buss, H. G.; Ellebracht, N. C.; Lynd, N. A.; Fischer, D. A.; Finlay, J.; Hill, S.; Callow, M. E.; Callow, J. A.; Kramer, E. J.; Zuckermann, R. N.; Segalman, R. A. *ACS Macro Lett.* **2014**, *3*, 364−368.

(20) Cao, Z.; Mi, L.; Mendiola, J.; Ella-Menye, J.-R.; Zhang, L.; Xue, H.; Jiang, S. *Angew. Chem., Int. Ed.* **2012**, *51*, 2602−2605.

(21) Chen, S.; Zheng, J.; Li, L.; Jiang, S. *J. Am. Chem. Soc.* **2005**, *127*, 14473−14478.

(22) Kyomoto, M.; Moro, T.; Yamane, S.; Watanabe, K.; Hashimoto, M.; Takatori, Y.; Tanaka, S.; Ishihara, K. *Biomaterials* **2014**, *35*, 6677−6686.

(23) Bodkhe, R. B.; Stafslien, S. J.; Daniels, J.; Cilz, N.; Muelhberg, A. J.; Thompson, S. E. M.; Callow, M. E.; Callow, J. A.; Webster, D. C. *Prog. Org. Coat.* **2014**, 369−380.

(24) Li, J.-H.; Li, M.-Z.; Miao, J.; Wang, J.-B.; Shao, X.-S.; Zhang, Q.-Q. *Appl. Surf. Sci.* **2012**, *258*, 6398−6405.

(25) West, S. L.; Salvage, J. P.; Lobb, E. J.; Armes, S. P.; Billingham, N. C.; Lewis, A. L.; Hanlon, G. W.; Lloyd, A. W. *Biomaterials* **2004**, *25*, 1195−1204.

(26) Zhang, Z. C. S.; Chang, Y.; Jiang, S. *J. Phys. Chem. B* **2006**, 10799.

(27) Iwasaki, Y.; Ishihara, K. *Anal Bioanal Chem.* **2005**, *381*, 534−546.

(28) Ishihara, K.; Ziats, N. P.; Tierney, B. P.; Nakabayashi, N.; Anderson, J. M. *J. Biomed. Mater. Res.* **1991**, *25*, 1397−1407.

(29) Ishihara, K.; Nomura, H.; Mihara, T.; Kurita, K.; Iwasaki, Y.; Nakabayashi, N. *J. Biomed. Mater. Res.* **1998**, *39*, 323−330.

(30) Ishihara, K.; Ueda, T.; Nakabayashi, N. *Polym. J.* **1990**, *22*, 355−360.

(31) Kiritoshi, Y.; Ishihara, K. *Polymer* **2004**, *45*, 7499−7504.

(32) Lee, H.; Alcaraz, M. L.; Rubner, M. F.; Cohen, R. E. *ACS Nano* **2013**, *7*, 2172−2185.

(33) Thouvenin, M.; Langlois, V.; Briandet, R.; Langlois, J. Y.; Guerin, P. H.; Peron, J. J.; Haras, D.; Vallee-Rehel, K. *Biofouling* **2003**, *19*, 177−186.

(34) Kerr, A.; Cowling, M. J. *Philos. Mag.* **2003**, *83*, 2779−2795.

DOI: 10.1021/mz500818c
ACS Macro Lett. 2015, 4, 505−510

(35) Hayden, H. S.; Blomster, J.; Maggs, C. A.; Silva, P. C.; Stanhope, M. J.; Waaland, J. R. *Eur. J. Phycol.* **2003**, *38*, 277−294.
(36) Zhang, S.; Zou, J.; Zhang, F.; Elsabahy, M.; Felder, S. E.; Zhu, J.; Pochan, D. J.; Wooley, K. L. *J. Am. Chem. Soc.* **2012**, *134*, 18467−18474.
(37) Zou, J.; Zhang, F.; Zhang, S.; Pollack, S. F.; Elsabahy, M.; Fan, J.; Wooley, K. L. *Adv. Healthcare Mater.* **2014**, *3*, 441−448.
(38) Xiong, M.-H.; Bao, Y.; Yang, X.-Z.; Wang, Y.-C.; Sun, B.; Wang, J. *J. Am. Chem. Soc.* **2012**, *134*, 4355−4362.

DOI: 10.1021/mz500818c
ACS Macro Lett. 2015, 4, 505−510